이학석사 학위논문

Spatiotemporal Interactome of piRNAs Recruiter Tudor and KH domain-containing protein (TDRKH) Revealed with Proximity Labeling in Cancer Cell Line

효소 화학반응을 통한 미토콘드리아 외막 단백질 TDRKH의
시공간적 상호작용체 분석

2020년 12월

서울대학교 대학원
자연과학대학 화학부
박준상

Spatiotemporal Interactome of piRNAs Recruiter Tudor and KH domain-containing protein (TDRKH) Revealed with Proximity Labeling in Cancer Cell Line

지도교수 이현우

이 논문을 박준상석사 학위논문으로 제출함

2020년 12월

서울대학교 대학원

자연과학대학 화학부

박준상

박준상의 석사 학위논문을 인준함

2020년 12월

위 원 장	서필준	(인)
부 위 원 장	이현우	(인)
위 원	김성연	(인)

Abstract

Joon-Sang Park
Department of Chemistry
The Graduate School
Seoul National University

Tudor and KH domain-containing protein (TDRKH) has been known for recruiting PIWI-interacting RNA (piRNA) precursor to mitochondria in the germline. Most of the studies regarding piRNAs has been conducted on germlines, however, TDRKH is also sufficiently expressed in the somatic tissues and cancer cell lines. To identify its interactome in the immortalized cell line, we introduced proximity labeling technique by fusing TurboID, an engineered promiscuous biotin ligase at the C-terminus of TDRKH. After confirmation that TDRKH-TurboID constructs are well expressed at the mitochondria, we analysed the biotinylated interactome of TDRKH-TurboID via Spot-BioID workflow. Our result reveals TDRKH may be involved in the messenger RNA (mRNA) processing at the surface of mitochondria with other RNA binding proteins (RBPs). We also observe that several cytoskeleton proteins interact with TDRKH and this result implies that TDRKH might be involved in the mitochondrial transport process. Among these proteins, surprisingly, HTT and SNCA which are highly expressed in the neuronal system and related to the Huntington disease and Parkinson' s disease are also observed in the interactome of TDRKH, this result might imply the relationship of TDRKH to its reported disease (i.e., hereditary motor neuropathies) and knockout phenotype in the mice (i.e., auditory brain stem response). We also conducted the domain-wise interactome

mapping of TDRKH by construction of deleted KH domain in the construct. Our result showed that SNCA is specific binder toward KH1 domain and SCRIB is specific binder toward KH2 and Tudor domain of TDRKH.

.....

keywords : TDRKH, proteomics, proximity labeling, TurboID, mitochondria
Student Number : 2019-27124

Table of Contents

I. Introduction

Mitochondria play a crucial role for generation of cellular energy (i.e. ATP) [1]. However, recent mitochondrial proteome mapping studies showed that many of proteins whose functions are not related to the cellular energy production [2]. For instance, anti-viral signaling is conducted via mitochondrial outer membrane anchored protein, MAVS, however, it is still not clearly understood why this process should be occurred at the outer mitochondrial membrane (OMM) and how this process can be coordinated with energy production, which is regarded as a main function of mitochondria.

Similarly, PIWI-interacting RNA (piRNA) maturation process is observed at the surface of mitochondria in germlines of C. elegans [3], insect [4], mice [5,6] and human [7]. Unlike miRNA or siRNA, piRNAs are transcribed into long piRNA precursor, and this precursor are matured at the OMM, by trimming and 2'-O-methylation [8]. The mature piRNA has a varied length from 26 to 31 nucleotide and piRNA inhibits the retrotransposon activity (e.g. LINE-1) and protect the genome integrity [9]. However, it is still rather puzzling why this piRNA maturation process is occurred at the OMM and how this process is coordinated with mitochondrial function.

Among the protein components which participate piRNA maturation [10], TDRKH, a mitochondrial protein [2] which is essential for spermatogenesis [5] is expressed not only expressed in the germline [4-6,11-13] but also expressed in the somatic tissue and cancer cell lines while other protein components in piRNA processing are solely expressed in the reproduction system [14]. In germline, TDRKH is known to recruit piRNA intermediate around 31 to 37 nucleotides and interacts with PIWI protein

(Figure 1B) [11,15], yet, this known molecular function of TDRKH may not reflect that of TDRKH in the cancer cell lines because the piRNA expression levels are negligible in various cancer cell lines which express the piRNA processing machinery including TDRKH detected in the recent study [14].

Among the somatic tissues, high expression level of TDRKH in the neuronal cells are observed in the transcriptomics level (https://gtexportal.org/home/gene/TDRKH, Figure 1A) and recent human genetics studies showed that TDRKH mutants are related to the survival of motor neuron [16] and the pathogenesis of hereditary motor neuropathies [17]. Mice knockout model of TDRKH is viable, however, it has a phenotype of the auditory brain stem response (https://www.mousephenotype.org/data/genes/MGI:1919884). TDRKH is also associated to the development of cancer such as chronic myelogenous leukemia and hepatocellular carcinoma and our group has recently discovered it in the proteome of mitochondrial associated membrane (MAM) of a human-derived immortalized cell line (i.e. HEK293T) (Figure 1C) [18]. Thus, it is reasonable to expect that TDRKH may have other molecular functions in the somatic cells or in the tissues which has not been described in the TDRKH studies in the germline [4-6,11-13].

II. Materials and methods

1. Cell culture and transfections

HEK293T were obtained from ATCC (Manassas, VA, USA), HEK293 Flip-in T-rex were obtained from Thermo Fisher Scientific. All cell lines were maintained in high glucose DMEM medium with 10% fetal bovine serum at 37° C in 5% CO2. All cell lines were transiently transfected at 60-80% confluence using turbofect (Invitrogen).

2. Expression plasmids and antibodies

Genes were cloned into the specified vectors using standard enzymatic restriction digest and ligation with T4 DNA ligase. To generate constructs where V5 epitope tag was appended to the protein, the tag was included in the primers used to PCR-amplify the gene. PCR products were digested with restriction enzymes and ligated into cut vectors (e.g. pCDNA3 and pCDNA5). The CMV promoter was used for expression in mammalian cells. Antibodies were used for western blotting and immunofluorescence imaging: anti-V5 (1:5000, Thermo Fischer), anti-TOM20 (1:1000, Proteintech), Alexa Fluor 647 conjugated Streptavidin (1:3000 dilutions, Invitrogen, cat no. S-21374), HRP conjugated Streptavidin (1:10000, Invitrogen). Alexa Fluor-conjugated anti-mouse, rabbit (1:3000, respectively, Invitrogen).

3. Construction of stably expressed TDRKH-V5-TurboID cell line

Flp-In™ T-REx™ 293 cells were cultured in DMEM (Gibco) supplemented with 10% FBS, 50 units/mL penicillin, and 50

□g/ml streptomycin at 37° C under 5% CO2. Stable cell lines were firstly generated by transfection with the pcDNA™5 expression construct plasmid expressing TDRKH-V5-TurboID. Cells were transfected at 60-80% confluence using TurboFect (Invitrogen). After 24 hr, cells were split into a 90 mm cell culture dish (SPL) with the proper concentration of Geneticin (G418) (500 μg/mL). After 2-3 weeks, 3-4 colonies were selected and transferred to a 24-well plate. Cells were continuously split into larger plates, and a cell stock was made. Expression was induced by 5 ng/mL doxycycline (Sigma Aldrich).

4. In situ biotinylation and immunoblotting

All cell lines were biotinylated with 50 μM of biotin (Alfa aesar) for 30 min. and lysed with RIPA buffer (ELPISBIO) containing 1× protease cocktail (Invitrogen) for 30 min at 4° C. Lysates were transferred to e-tube and vortexed for 2 min. And lysates were clarified by centrifugation at 15,000g for 10 min at 4° C. The lysates were loaded by boiling at 95° C for 5 min after 1x SDS-PAGE loading buffer. After that, the proteins were resolved by SDS-PAGE.

5. Immunofluorescence

To visualize the subcellular localization of the transiently expressing POI, cells were plated on coverslips (thickness no. 1.5 and radius: 12 mm). For fixed cell imaging, cells were fixed by 4% paraformaldehyde and permeabilized with cold methanol for 5 min at −20° C. Next, cells were washed with Dulbecco's phosphate-buffered saline (DPBS) and blocked for 1 h with 2%

BSA in DPBS at room temperature. Immunolabeling was conducted in blocking solution with proper diluted antibodies—anti-V5 antibodies and anti-TOM20 antibodies — and Alexa-labelled secondary antibodies (mouse anti-Alexa 488 antibodies, rabbit anti-Alexa 568 antibodies and anti-streptavidin Alexa 647 antibodies)

6. Proteome digestion and enrichment of biotinylated peptides

TDRKH-V5-TurboID stable cells were grown in three T75 flasks for triplicate mass analysis per one condition. After 24 hr doxycycline treatment, 50 μM of biotin was added for biotinylation. After 30min labeling, the cells were washed three times with DPBS and then lysed with 1.5 mL 2% SDS in 1× TBS (25 mM Tris, 0.15 M NaCl, pH 7.2, Thermoscientific, 28358), 1 × protease inhibitor cocktail. Lysates were clarified by ultrasonication (Bioruptor, diagenode) for 15 min with cold water bath. For removal of free biotin, 6 times the sample volume of cold acetone -S35- (-20° C, Sigma-Aldrich, 650501) was added to each lysate and kept at -20° C. After at least two hours, samples were centrifuged at 13,000 × g for 10 min at 4° C. Supernatant was removed gently. 6.3 mL of cold acetone and 700 μL of 1× TBS were added to pellet. Samples were vortexed vigorously and kept at -20° C. After overnight, samples were centrifuged at 13,000 × g for 10 min at 4° C. Supernatant was removed gently. Allow pellet to air dry for 5min. Pellet was resolubilized with 1 mL of 8 M urea (Sigma-Aldrich) in 50 mM ammonium bicarbonate (ABC, Sigma-Aldrich). Concentration of protein was measured by BCA assay. Samples were denatured at 650 rpm for 1 h at 37° C

using Thermomixer (Eppendorf). The samples were reduced by adding dithiothreitol (Sigma-Aldrich) to 10 mM final concentration and incubated at 650 rpm for 1 h at 37° C using Thermomixer. The samples were alkylated by adding iodoacetamide (Sigma-Aldrich) of 40 mM to final concentration and mixed at 650 rpm for 1 h at 37° C using Thermomixer. The samples were diluted eight times using 50 mM ABC. CaCl2 (Alfa aesar) was added to 1 mM final concentration. Trypsin (Thermoscientific) was added to each sample (1:50 w/w). Samples were incubated at 650 rpm for 6-18 h at 37° C using Thermomixer. Samples were centrifuged at 10,000 × g for 3 min to remove insoluble material. Then, 300 μL of streptavidin beads (Pierce) was washed with 2 M urea in 1× TBS for four times and added to the sample. The samples were rotated for 1 h at room temperature. The flow-through fraction was kept, and the beads were washed twice with 2 M urea in 50 mM ABC. After removing the supernatant, the beads were washed with pure water in new tubes. Biotinylated peptides were heated at 60° C and mixed at 650 rpm after adding 500 μL 80% acetonitrile (Sigma-Aldrich), 0.2% TFA (Sigma-Aldrich), and 0.1% formic acid (Thermoscientific). Each supernatant was transferred to new tubes. Repeat elution step four more times. Combined elution fractions were dried using Speed vac (Eppendorf).

III. Results

1. TDRKH is a transmembrane protein facing to the cytosol at the outer mitochondrial membrane.

Using TMHMM algorithm, we could observe that TDRKH has a strongly predicted single transmembrane domain (17-34 aa) at the N-terminus (Figure 1D). Thus, we expect that the rest part (from 35aa to C-terminus) of TDRKH should be exposed at the cytosolic face at the OMM. It is noteworthy that the lysine residues in this predicted cytosol-exposed part of TDRKH were labeled by Contact-ID which conducts in situ biotinylation on the cytosol-exposed lysine residues of MAM-localized proteins [18].

To validate the membrane topology of TDRKH at the OMM, we employed the APEX-method [19]. APEX2 was tagged at the C-terminus of TDRKH and TDRKH-V5-APEX2 construct was expressed in the HEK293T cells. As shown in Figure 1E, TDRKH-V5-APEX2 showed a good mitochondria pattern (i.e. anti-V5 immunofluorescence) and well merged with mitochondrial marker protein, Mito-BFP while its biotinylated pattern is quite diffusive to the cytosol (i.e. Streptavidin-AF647) and this result indicated that APEX2 should not be in the membrane-restricted region [20]. To confirm its correct localization in the mitochondria, we conducted electron microscope imaging via APEX-DAB staining method [21]. As shown in the Figure 1F, it is clearly shown that APEX2-DAB stain is shown at the cytosolic face of mitochondria and this result confirms our proposed membrane topology of TDRKH at the outer mitochondrial membrane (Figure 1C).

A

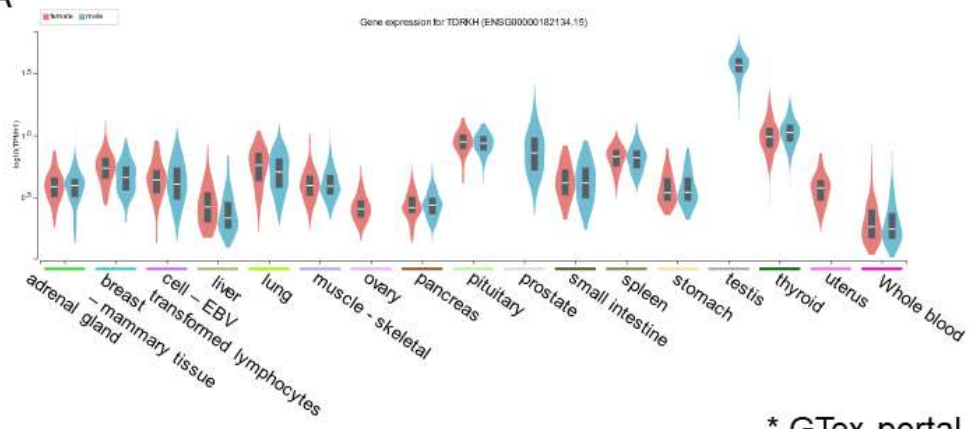

* GTex portal

B

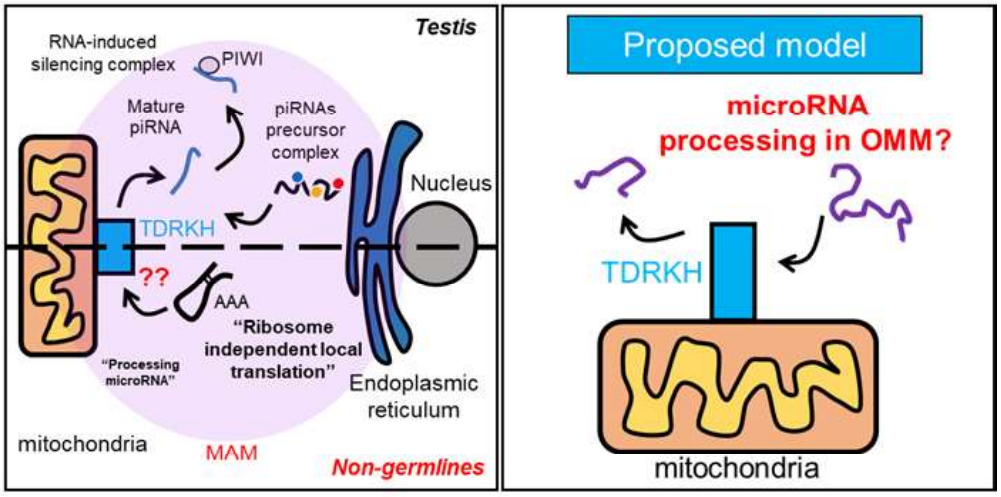

C

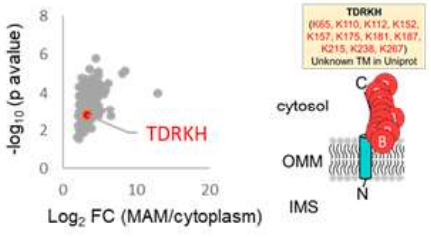

D

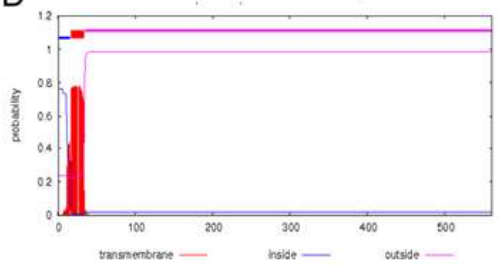

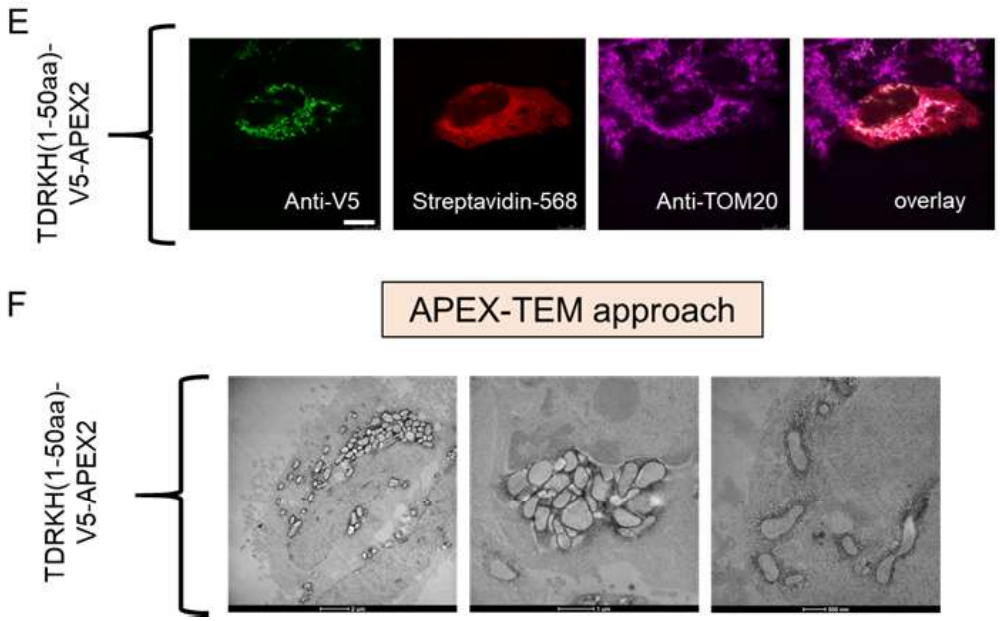

Figure 1. TDRKH distribution and studies. (A) TDRKH protein expression distribution. Expression level is variable in several different tissues, including testis, lung, and gallbladder. Data from GTExPortal (https://gtexportal.org/home/gene/TDRKH). (B) Graphical depict of piRNA biogenesis and mechanism regarding TDRKH (left). Proposed model of TDRKH regarding RNA processing in mitochondrial outer membrane. (C) TDKRH identification in MAM, facing cytosol with its C-terminus domain. (D) TMHMM prediction of TDRKH indicates the N-terminal localization of transmembrane domain (http://www.cbs.dtu.dk/services/TMHMM/). (E) Confocal image of N-terminus of TDRKH (1-50AA) indicates it is sufficient for targeting mitochondrial outer membrane. TDRKH 1-50AA (green), biotinylation of TDRKH 1-50 AA (red), TOM20 (violet). (F) TEM image of N-terminus TDKRH suggests its targeting of mitochondrial outer membrane.

2. Proteomic mapping of TDRKH interactome in live mammalian cell by using proximity labeling method

To discover the molecular interactome of TDRKH in live cells, we introduced a proximity labeling tool. We utilized TurboID [22], a fast-kinetics engineered version of BioID which labels proximal proteins via in situ generated biotin-AMP ester. Since bioin-AMP ester can covalently attach on the lysine residues of proximal proteins within 50 nanometer, TurboID can selectively biotinylate the proximal proteins or interaction proteins with TDRKH when we genetically express TurboID with TDRKH in live cells. (Figure 2A).

TDRKH has two K Homology domains (KH1 and KH2) which have RNA binding affinity [23] and one Tudor domain which has a binding affinity toward demethylated arginine residue[11] (Figure 2B). We cloned TDRKH-V5-TurboID whose TurboID is conjugated at the cytosol-exposed C-terminus domain of TDRKH. Thus, we expect that it can reveal the interactome of TDRKH at the cytosolic face of mitochondria (Figure 2A & B). In confocal microscope imaging results with HEK293T cells, TDRKH-V5-TurboID was well localized in mitochondria and its pattern (i.e. anti-V5 immunofluorescence) is nicely overlapped with immunofluorescence pattern of TOM20, a mitochondrial marker protein (Figure 2C). Also, biotinylated protein patterns of TDRKH-V5-TurboID was also well-overlapped with anti-TOM20 pattern (Figure 2C).

For controlling its expression and minimizing artifacts from the transient overexpression issue from transfection, we generated doxycycline-inducible stable cell line of

TDRKH-V5-TurboID using Flip-In HEK293T-Rex cell line. Using this stable cell line of TDRKH-V5-TurboID, we could see that the biotinylated interactome proteins were reproducibly generated by Streptavidin-HRP western blot analysis (Figure 2D). We confirmed that these biotinylated proteins were successfully enriched by Streptavidin-magnetic bead which is an essential step for the mass analysis (Figure 2D).

For the mass analysis of biotinylated proteins by TDRKH-V5-TurboID, we employed Spot-BioID method [18, 24] which directly profiles the biotinylated proteins by detection of the post-translational modification of biotin (K+226 Da) on the biotinylated peptides. This method is the most correct method to detect the biotinylated proteome by BioID or TurboID compared to other widely used "indirect" method to detect unlabeled peptides from streptavidin bead enrichment. While this indirect method cannot guarantee whether their mass-detected peptides are really biotinylated, our Spot-BioID workflow perform the most correct identification of the biotinylated proteins of TurboID (Figure 3A).

Since TurboID of TDRKH-TurboID is exposed at the cytosol, we utilized cytosolic TurboID (TurboID-NES) as a control sample for our analysis. By following of Spot-BioID method, total 690 non-redundant biotinylated sites and 445 biotinylated proteins were identified in the biological triplicate samples of TDRKH-V5-TurboID cell line while TurboID-NES labels 2595 proteins. By filtering them with cytosolic control, we could acquire 45 biotinylated protein with 65 non-redundant biotinylated sites that can be regarded as TDRKH interactome (Figure 3B). Among these proteins, 16 proteins were overlapped

with MAM proteome of human testes [25] and 7 proteins are covered with our recently mapped MAM proteome in HEK293T cells [18], These overlaps with MAM proteome findings propose TDRKH' s localization at the MAM [18]. All of 45 TDRKH interactome is shown in Figure 3C. Since TDRKH is an OMM protein, several known outer mitochondrial membrane proteins (e.g. MAVS, FKBP8, AKAP1, EXD2) were mapped along with several ER membrane proteins (UBXN4, PTPN1, SSR) and many cytosolic proteins (Figure 3C).

Interestingly, our TDRKH interactome can be clustered with the similar molecular functions which are also related to the physiological processes at the MAM: protein degradation (e.g. UBXN4, PTPN1, HSPA1B, CDCA3, USP7), endocytic control (e.g. AAGAB, HTT), immune response (e.g. MAVS, ZC3HAV1, DDX3X, AKAP1), RNA processing (e.g. AKAP1, EEF1A1P5, NRBF2, EXD2, EIF4G1, DCLRE1A, LARP4, ENPP1, DOCK7, PABPC1), cell organization (e.g, MTFR1, STMN1, CTTN, CEP350, MAP4, SCRIB, PKN3, TBC1D15, SYAP1, KIAA0100, OCIAD1, DNM1L, ATPAF1, PAK4, TES), and apoptosis (e.g., FKBP8) (Figure 3D). Thus, our findings could reflect that TDRKH may modulate diverse processes with interactome at the OMM and at the MAM of somatic cell lines.

Yet TDRKH is a mitochondrial protein, comparison with TOM20 interactome or FKBP8 interactome could grant us to have a new point of view with TDRKH and its mitochondrial interactome. TOM20 shares around 25% of its interactome with TDRKH, and FKBP8 shares about 15% of its interactome. Since the viral process and programmed cell death are known to be related with mitochondria, we looked for proteins annotated for

these proteins are whether labeled in TOM20 or FKBP8 interactome. Surprisingly, the proteins annotated for those functions were scarcely found in TOM20 or FKBP8, suggesting these functions are more likely to be TDRKH-specific.

Interestingly, alpha-synuclein (SNCA) and Huntington protein (HTT) are shown in 45 interactome protein of TDRKH. Since these proteins are not overlapped with an interactome result of FKBP8 which is an cytosolic exposed OMM- and MAM protein (Supplemental Figure 1). Because both proteins are related to the neurodegenerative diseases (e.g. Parkinson's disease, Huntington's disease), it might be intriguing how TDRKH can modulate these protein function in the pathological process of neurodegenerative diseases.

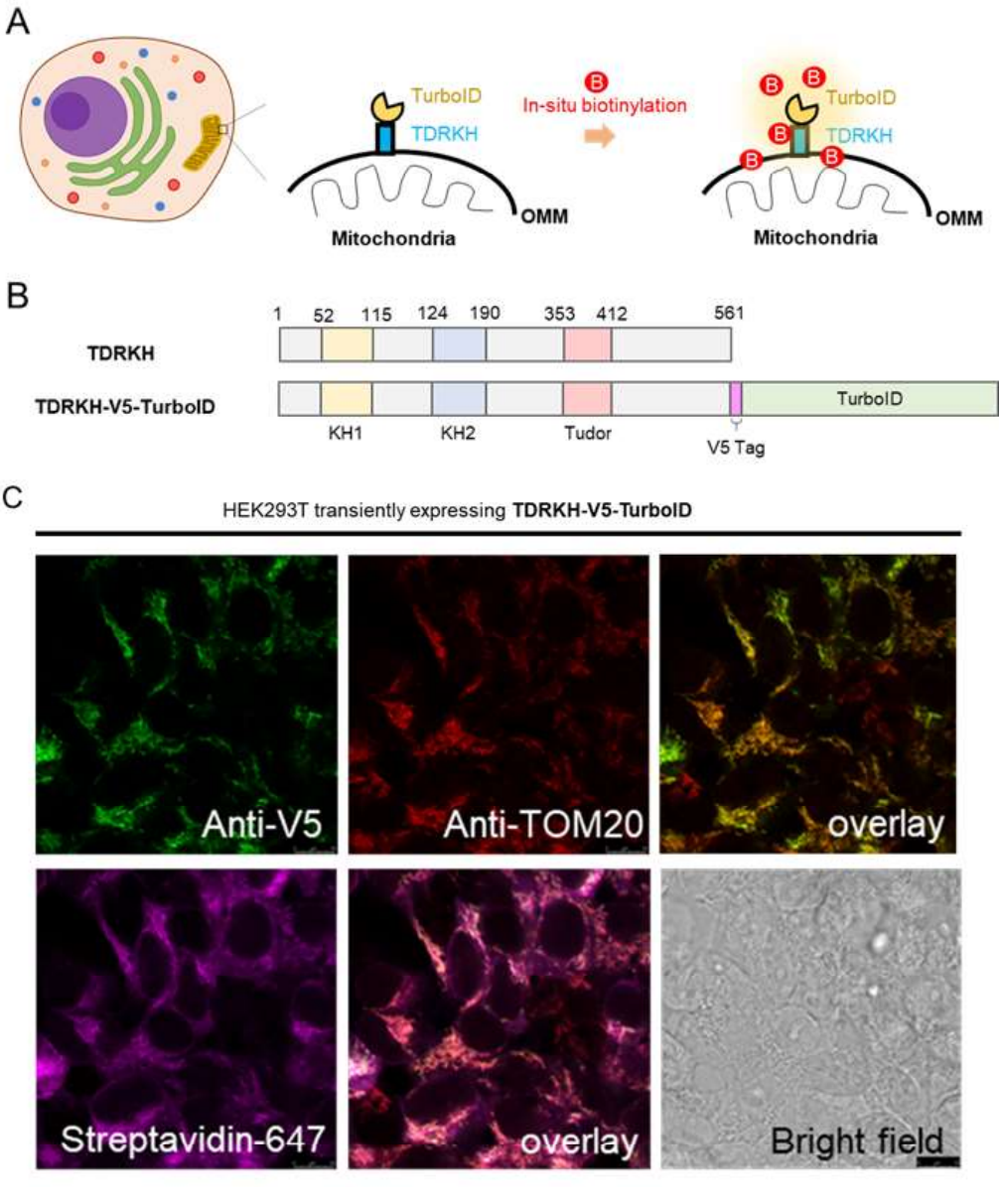
A
TurboID
TDRKH
OMM
Mitochondria
In-situ biotinylation
TurboID
TDRKH
OMM
Mitochondria
B
1
52
115
124
190
353
412
561
TDRKH
TDRKH-V5-TurboID
TurboID
KH1
KH2
Tudor
V5 Tag
C
HEK293T transiently expressing TDRKH-V5-TurboID
Anti-V5
Anti-TOM20
overlay
Streptavidin-647
overlay
Bright field

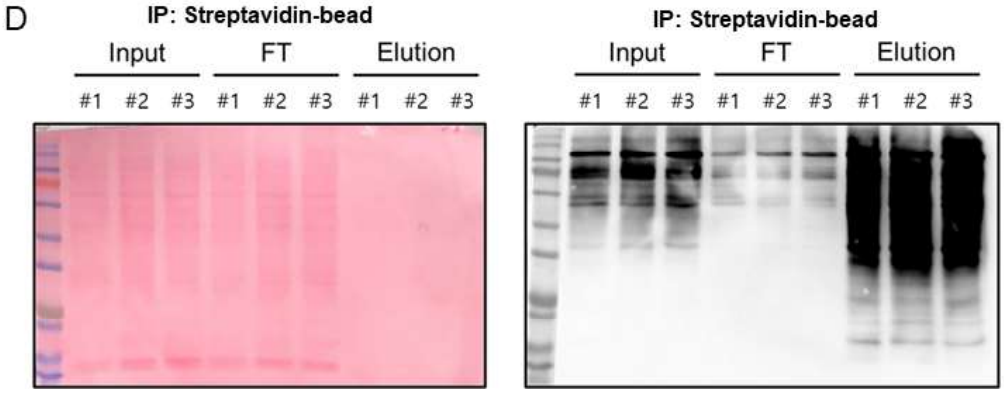

Figure 2. Production of recombinant TDRKH and in-situ biotinylation. (A) Graphical depict of TDRKH interactome labeling process. Biotinylation via TurboID and exogenous biotin. TurboID labeling radius is visualized as yellow circle. Biotin is shown as red dot. (B) Domain architecture of wild-type TDRKH. TDRKH consist of two K Homology domain (KH1 and KH2, yellow and blue, respectively), and one Tudor domain (red) (up). Recombinant TDRKH-V5-TurboID. Epitope tag V5 (pink) and TurboID (green) were fused into C-terminus of TDRKH (down). (C) Localization and biotinylation of recombinant TDRKH. TDRKH (green), TOM20 (red), biotinylation (violet). (D) Streptavidin bead enrichment of biotinylated TDRKH interactome. (Left: Ponceau S staining, Right: SA-HRP)

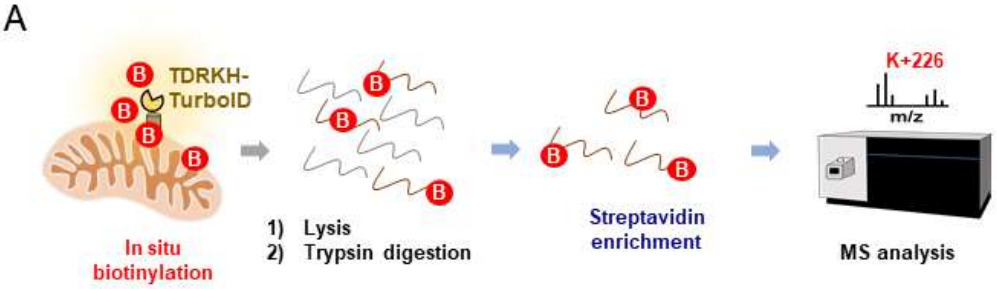
A
TDRKH-
TurboID
In situ
biotinylation
1) Lysis
2) Trypsin digestion
Streptavidin
enrichment
K+226
m/z
MS analysis

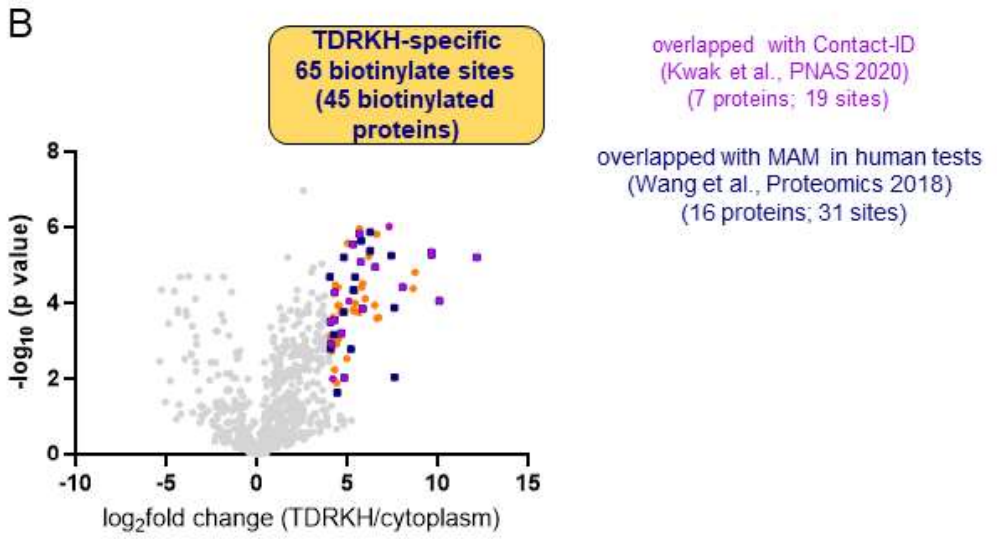
B
TDRKH-specific
65 biotinylate sites
(45 biotinylated
proteins)
overlapped with Contact-ID
(Kwak et al., PNAS 2020)
(7 proteins; 19 sites)
overlapped with MAM in human tests
(Wang et al., Proteomics 2018)
(16 proteins; 31 sites)
-log10 (p value)
log2fold change (TDRKH/cytoplasm)

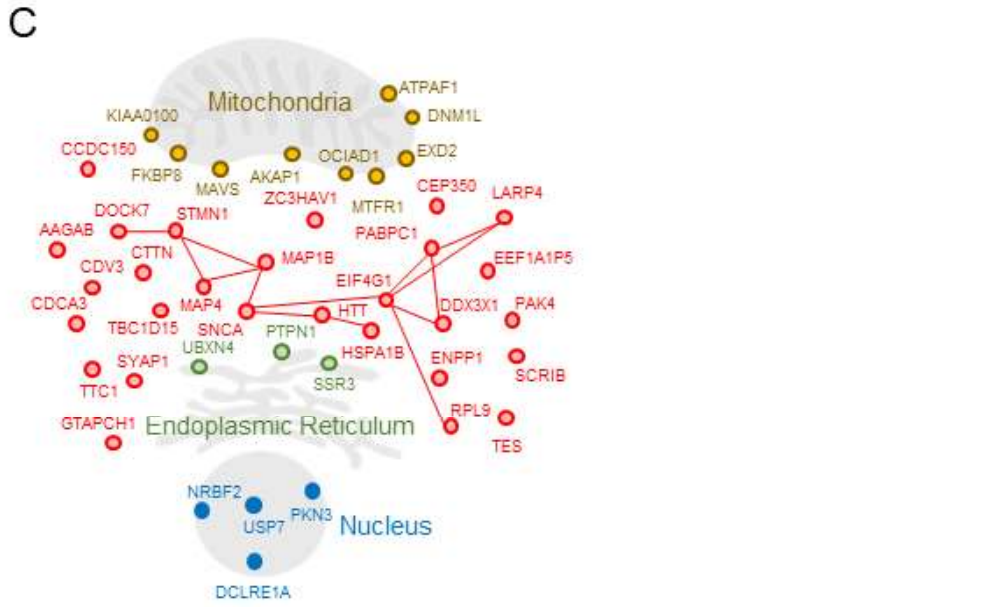
C
Mitochondria
Endoplasmic Reticulum
Nucleus
ATPAF1
DNM1L
KIAA0100
CCDC150
FKBP8
MAVS
AKAP1
OCIAD1
EXD2
CEP350
LARP4
ZC3HAV1
MTFR1
DOCK7
STMN1
AAGAB
PABPC1
CTTN
CDV3
MAP1B
EEF1A1P5
EIF4G1
CDCA3
MAP4
HTT
DDX3X1
PAK4
TBC1D15
SNCA
PTPN1
UBXN4
HSPA1B
ENPP1
SCRIB
SYAP1
SSR3
TTC1
RPL9
GTAPCH1
TES
NRBF2
PKN3
USP7
DCLRE1A

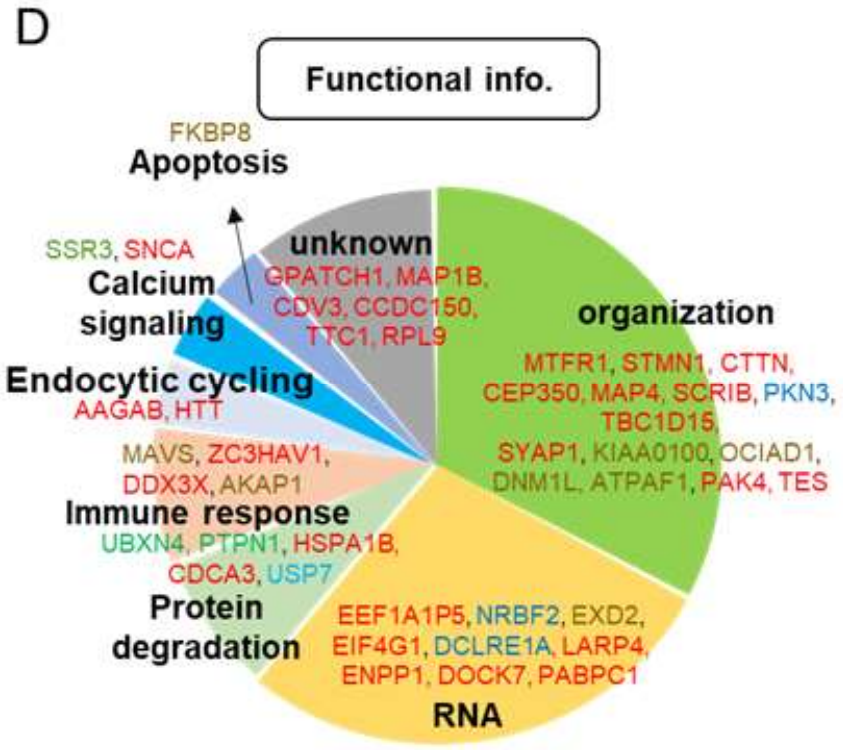

Figure 3. Production of recombinant TDRKH and in-situ biotinylation. (A) Graphical depict of mass sampling process of TDRKH interactome and its analysis. (B) Volcano plot of TDRKH interactome compared with NES interactome (cytoplasmic proteins) reveals 45 TDRKH specific interactome. (C) Subcellular distribution 45 TDRKH interactome. Red line data from STRING interaction. (D) Functions of 45 TDRKH interactome shown in pi chart.

3. Domain-deleted interactome mapping reveal unexpected interactome of KH domains of TDRKH.

Since TDRKH has two RNA-binding KH domains and Tudor domain which is also related to the RNA binding, TDRKH has been acknowledged as a piRNA precussor recruiter to the OMM [5]. Our mass analysis result also showed that many RNA binding proteins (e.g., AKAP1, EEF1A1P5, NRBF2, EXD2, EIF4G1, DCLRE1A, LARP4, ENPP1, DOCK7, PABPC1) were enriched in TDRKH-TurboID sample which supports that TDRKH may participate in the RNA processing mechanism at the OMM. To examine whether TDRKH can interact with these RBPs by complexation with RNA molecules, we prepared the each single domain (KH1, KH2 and Tudor) deleted constructs of TDRKH-TurboID (Figure 4A). We confirmed that each domain-deleted constructs are well expressed at the mitochondria and their in situ biotinylating activity is not compromised by deletion of the domain (Figure 4B & C).

We conducted mass analysis of biological triplicate samples of each domain-deleted TDRKH-TurboID constructs, respectively, by following Spot-BioID workflow. The identified biotinylated peptidome results were compared with full TDRKH-TurboID result (Figure 5A-C). From this analysis, we could find that ENPP1 and SNCA are not shown in KH1-deleted construct result and SCRIB and IGBP1 are not shown in the result of KH2-deleted construct. In the Tudor-domain deleted construct sample, SERBP1 and SCRIB are not shown compared to the interactome result of full TDRKH-TurboID. These results propose that each domain may have preferential interaction partner proteins.

Among these proteins, alpha-synuclein (SNCA) and SCRIB which is known scaffold protein involved in different aspects of polarized cell differentiation regulating epithelial and neuronal morphogenesis are shown in KH1 and KH2 domain specific interaction partner, respectively. Since these proteins are not well-known RBPs, it might be interesting to characterize how these proteins interact with KH domain of TDRKH in further study.

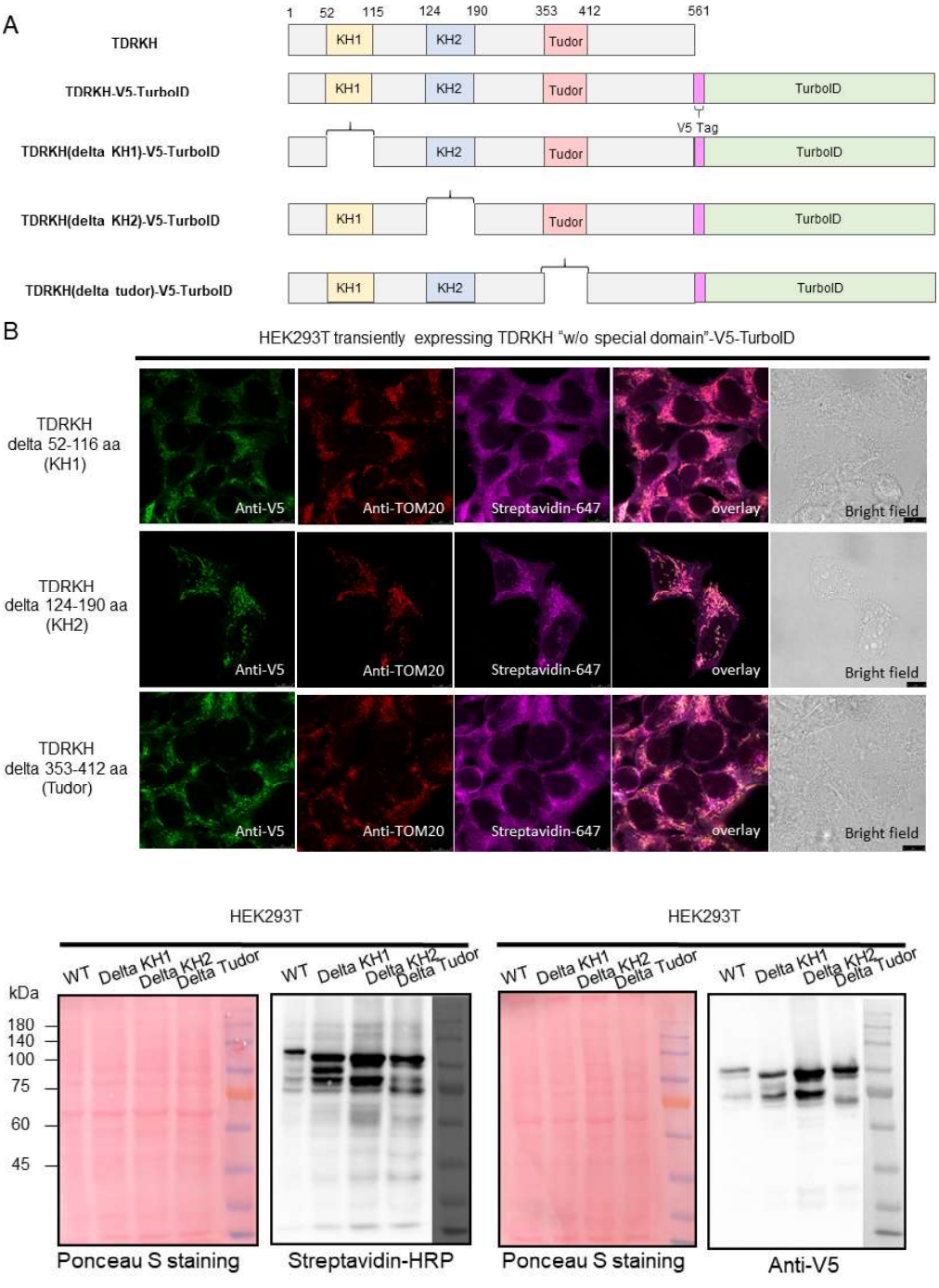
A
1
52
115
124
190
353
412
561
TDRKH
TDRKH-V5-TurboID
TDRKH(delta KH1)-V5-TurboID
TDRKH(delta KH2)-V5-TurboID
TDRKH(delta tudor)-V5-TurboID
KH1
KH2
Tudor
TurboID
V5 Tag
B
HEK293T transiently expressing TDRKH "w/o special domain"-V5-TurboID
TDRKH delta 52-116 aa (KH1)
TDRKH delta 124-190 aa (KH2)
TDRKH delta 353-412 aa (Tudor)
Anti-V5
Anti-TOM20
Streptavidin-647
overlay
Bright field
HEK293T
HEK293T
WT
Delta KH1
Delta KH2
Delta Tudor
kDa
180
140
100
75
60
45
Ponceau S staining
Streptavidin-HRP
Ponceau S staining
Anti-V5

Figure 4. Production and analysis of domain specific TDRKH interactome. (A) Domain architecture of domain deleted TDRKH mutants. (B) Confocal image of TDRKH mutants also targets mitochondrial outer membrane. TDRKH mutants (green), TOM20 (red), biotinylation (violet). (C) Western blot analysis of TDRKH mutants in human cell (HEK293T). Biotinylation pattern (Streptavidin-HRP, lef) and TDRKH mutants (V5, right).

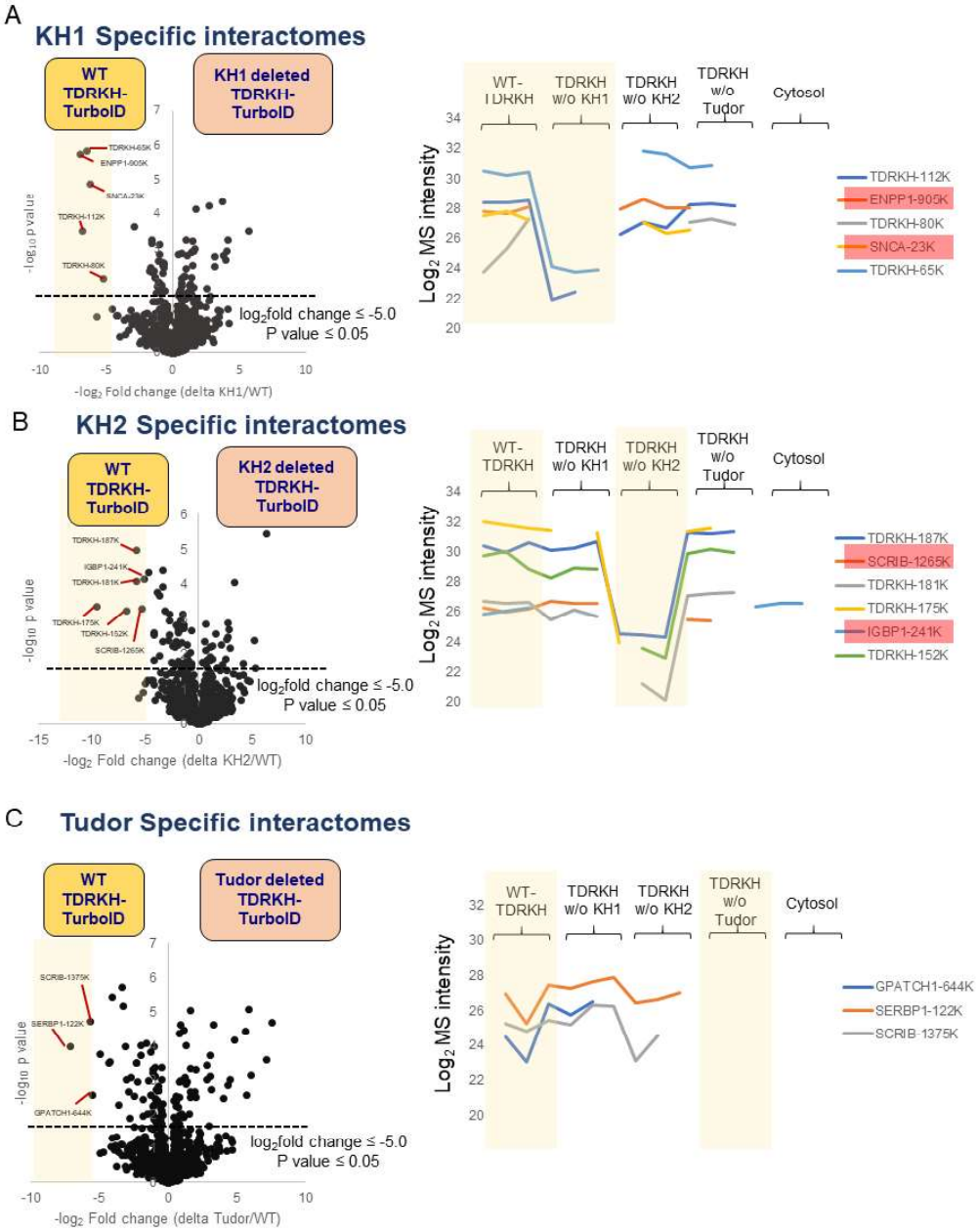

Figure 5. Analysis of domain specific TDRKH interactome. (A) Volcano plot of TDRKH and its KH1 domain deleted interactomes. (F) Volcano plot of TDRKH and its KH2 domain deleted interactomes. (G) Volcano plot of TDRKH and its tudor domain deleted interactomes.

IV. Discussion

In this study, we report our Spot-TurboID discovers other possible function of TDRKH in somatic or cancer cells. Although the protein has been known to process or regulate piRNA in germlines, endogenous levels of TDRKH are still high in other cell lines or tissue (Figure 1A). However, it is unclear what role this protein plays in other cells. Therefore, our proteomic results could be proposed for possible features of them at the ER-mitochondrial interfaces. Furthermore, we confirmed our domain-deleted interactome mapping unveiled KH domains might be interacted with neuronal factors (e.g. SNCA) in the HEK293 cell line [26], suggesting that HEK293 are originated to neuronal cell lines through previous genomic and transcriptomic results. However, further investigations should be required for deeply understanding the features.

We further show TDRKH-domain interactomes are clearly distinguished in mouse testis-based cell line (TM3, supplementary figure 2). We could propose that our own analysis of proximity labeling enables us precise information of interactome with target protein. Thereby, further study may precisely enlighten domain-based interactomes in all environments such as neuronal, testicular, and other cancer cells. Therefore, our analysis is valuable in that it has provided a clue to proceeding more precise biological study.

V. Reference

[1] L. D. Osellame, T. S. Blacker, M. R. Duchen, Best Pract Res Clin Endocrinol Metab 2012, 26, 711-723.

[2] S. Rath, R. Sharma, R. Gupta, T. Ast, C. Chan, T. J. Durham, R. P. Goodman, Z. Grabarek, M. E. Haas, W. H. W. Hung, P. R. Joshi, A. A. Jourdain, S. H. Kim, A. V. Kotrys, S. S. Lam, J. G. McCoy, J. D. Meisel, M. Miranda, A. Panda, A. Patgiri, R. Rogers, S. Sadre, H. Shah, O. S. Skinner, T. L. To, M. A. Walker, H. Wang, P. S. Ward, J. Wengrod, C. C. Yuan, S. E. Calvo, V. K. Mootha, Nucleic Acids Res 2021, 49, D1541-d1547.

[3] H. C. Lee, W. Gu, M. Shirayama, E. Youngman, D. Conte, Jr., C. C. Mello, Cell 2012, 150, 78-87.

[4] N. Izumi, K. Shoji, Y. Sakaguchi, S. Honda, Y. Kirino, T. Suzuki, S. Katsuma, Y. TOMari, Cell 2016, 164, 962-973.

[5] J. P. Saxe, M. Chen, H. Zhao, H. Lin, Embo j 2013, 32, 1869-1885.

[6] D. Ding, J. Liu, K. Dong, A. F. Melnick, K. E. Latham, C. Chen, Nucleic Acids Res 2019, 47, 2594-2608.

[7] Z. Williams, P. Morozov, A. Mihailovic, C. Lin, P. K. Puvvula, S. Juranek, Z. Rosenwaks, T. Tuschl, Cell Rep 2015, 13, 854-863.

[8] E. M. Weick, E. A. Miska, Development 2014, 141, 3458-3471.

[9] J. Casta□eda, P. Genzor, A. Bortvin, Mutat Res 2011, 714, 95-104.

[10] S. Hirakata, M. C. Siomi, Biochim Biophys Acta 2016, 1859, 82-92.

[11] C. Chen, J. Jin, D. A. James, M. A. Adams-Cioaba, J. G.

Park, Y. Guo, E. Tenaglia, C. Xu, G. Gish, J. Min, T. Pawson, Proc Natl Acad Sci U S A 2009, 106, 20336-20341.
[12] F. Mohn, D. Handler, J. Brennecke, Science 2015, 348, 812-817.
[13] M. Tan, H. Tol, D. Rosenkranz, E. F. Roovers, M. J. Damen, T. A. E. Stout, W. Wu, B. A. J. Roelen, Cells 2020, 9.
[14] P. Genzor, S. C. Cordts, N. V. Bokil, A. D. Haase, Proceedings of the National Academy of Sciences 2019, 116, 11111.
[15] J. C□t□, S. Richard, J Biol Chem 2005, 280, 28476-28483.
[16] S. Miura, K. Kosaka, T. Nomura, S. Nagata, T. Shimojo, T. Morikawa, R. Fujioka, M. Harada, T. Taniwaki, H. Shibata, Eur J Med Genet 2019, 62, 103594.
[17] M. F. Dohrn, M. Saporta, Curr Opin Neurol 2020, 33, 568-574.
[18] C. Kwak, S. Shin, J.-S. Park, M. Jung, T. T. M. Nhung, M.-G. Kang, C. Lee, T.-H. Kwon, S. K. Park, J. Y. Mun, J.-S. Kim, H.-W. Rhee, Proceedings of the National Academy of Sciences 2020, 117, 12109.
[19] C.-M. Yoo, H.-W. Rhee, Biochemistry 2020, 59, 250-259.
[20] S. Y. Lee, M. G. Kang, J. S. Park, G. Lee, A. Y. Ting, H. W. Rhee, Cell Rep 2016, 15, 1837-1847.
[21] J. D. Martell, M. Yamagata, T. J. Deerinck, S. Phan, C. G. Kwa, M. H. Ellisman, J. R. Sanes, A. Y. Ting, Nat Biotechnol 2016, 34, 774-780.
[22] K. F. Cho, T. C. Branon, N. D. Udeshi, S. A. Myers, S. A. Carr, A. Y. Ting, Nature Protocols 2020, 15, 3971-3999.

[23] F. S. Lamb, T. J. Barna, C. Goud, I. Marenholz, D. Mischke, B. C. Schutte, Gene 2000, 246, 209-218.
[24] S.-Y. Lee, H. Lee, H.-K. Lee, S.-W. Lee, S. C. Ha, T. Kwon, J. K. Seo, C. Lee, H.-W. Rhee, ACS Central Science 2016, 2, 506-516.
[25] X. L. Wang, Y. J. Wen, J. Dong, C. C. Cao, S. Q. Yuan, Proteomics 2018, 18.
[26] M. Orth, S. J. Tabrizi, A. H. Schapira, J. M. Cooper, Neurosci Lett 2003, 351, 29-32.

VI. Appendix

Protein	Gene names	Peptide sequence	Labeled site	Domain Specific
5VTE0	EEF1A1P5	AAGAGKVTK	450	
Q14318	FKBP8	AALKLEPSNK	334	
Q7Z434	MAVS	AGMVPSKVPTSMVLTK	362	
Q9Y2W6	TDRKH	AKAAIHQILTENTPVSEQLSVPQR	112	
Q15390	MTFR1	ANAGKTLVK	223	
Q7Z2W4	ZC3HAV1	ARPPSGSSKATDLGGTSQAGTSQR	314	
P16949	STMN1	DKHIEEVRK	128	
Q9BRR8	GPATCH1	DKYSVFNFLTLPETASLPTTQASSEK	644	Tudor
P46821	MAP1B	DSGGKTPGDFSYAYQKPEETTR	1863	
Q14247	CTTN	DYSKGFGGK	193	
Q5VT06	CEP350	EGKSDVLLK	2280	
Q9Y2W6	TDRKH	EVAAAKHLILEK	187	
P27816	MAP4	EVALVKDVR	318	
Q96F24	NRBF2	FAANTGKAK	254	
Q9Y2W6	TDRKH	GGGDMAVVVSKEGSWEKPSDDSFQK	267	
Q9NVH0	EXD2	GIGELVSEEPFVVKLR	396	
O00571	DDX3X	GKSSFFSDR	81	
Q04637	EIF4G1	GLPLVDDGGWNTVPISKGSRPIDTSR	1059	
Q14160	SCRIB	GLQPLKLDYR	1265	KH2, Tudor
Q9UKY7	CDV3	GRDEVSKNQALK	232	
Q92667	AKAP1	GVLFSSKSAEVCK	160	
Q6P5Z2	PKN3	IKEGVENLRR	34	
Q92575	UBXN4	IKQQIALDR	269	
P18031	PTPN1	ILEPHNGKCR	323	
Q6PJP8	DCLRE1A	ILPSGLKYNAR	543	

Protein	Gene names	Peptide sequence	Labeled site	Domain Specific
Q9Y2W6	TDRKH	ISGTQKEVAAAK	181	
Q71RC2	LARP4	ISRPHPSTAESKAPTPK	471	
Q9Y2W6	TDRKH	ITCDKESEGTLLLSR	162	
P54652	HSPA1B	ITITNDKGR	510	
Q8TC07	TBC1D15	KDSSSVVEWTQAPK	68	
P22413	ENPP1	KEPVSDILK	905	KH1
Q7Z2W4	ZC3HAV1	KGTGLLSSDYR	401	
Q8NCX0	CCDC150	KIRQELENR	984	
Q9Y2W6	TDRKH	KQPISVR	215	
Q9Y2W6	TDRKH	KQTGAR	80	
Q96A49	SYAP1	KFVEEQHTKK	119	
Q96A49	SYAP1	KFVEEQHTKK	118	
Q6PD74	AAGAB	KVHAEKVAK	290	
Q9Y2W6	TDRKH	LIKISGTQK	175	
Q14667	KIAA0100	LKSATGSEVR	2184	
Q99614	TTC1	LKEEMLGKLK	250	
Q9Y2W6	TDRKH	LTHCADWKPLVAK	449	
P32969	RPL9	NFLGEKYIR	121	
Q99618	CDCA3	QGKRPSPLSENVSELK	219	
Q9UNL2	SSR3	REDAVSKEVTR	98	
Q9NX40	OCIAD1	RKNITYEELR	195	
Q7Z2W4	ZC3HAV1	RKTVFSPTLPAAR	374	
Q9Y2W6	TDRKH	SICKASGAK	152	
Q96N67	DOCK7	SIIGSKGLDR	922	
O00429	DNM1L	SKPIPIMPASPQK	608	
O00429	DNM1L	SKPIPIMPASPQKGHAVNLLDVPVPVAR	619	
Q7Z2W4	ZC3HAV1	SLNYKSTSSGHR	448	
Q5TC12	ATPAF1	TDALGKQSVNR	131	
P37840	SNCA	TKQGVAEAAGK	23	KH1

Protein	Gene names	Peptide sequence	Labeled site	Domain Specific
P11940	PABPC1	TVPQYKYAAGVR	512	
O96013	PAK4	VHTGFDQHEQKFTGLPR	31	
Q14318	FKBP8	VKCLNNLAASQLK	273	
Q15390	MTFR1	VLFGPHMLKPTGK	318	
Q14160	SCRIB	VPQAEGPPKR	1375	KH2, Tudor
Q9Y2W6	TDRKH	VPQEAVKLIIGR	65	
Q7Z434	MAVS	VPTSMVLTKVSASTVPTDGSSR	371	
P42858	HTT	VSTQLKTNLTSVTK	1402	
Q5VTE0	EEF1A1P5	VTKSAQK	453	
Q9UGI8	TES	YTTLIAKLK	80	
Q93009	USP7	YTYLEKAIK	1096	

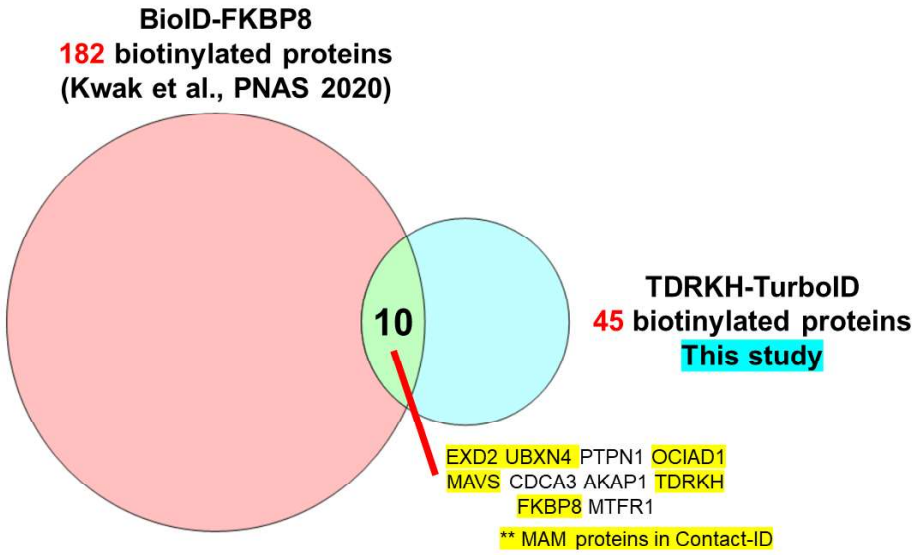

Supplementary Figure 1. Comparison of this proteomes with FKBP8 interactomes. Venn diagram showing overlap of proteins analyzed in the study and previous study (Kwak et al., PNAS 2020)

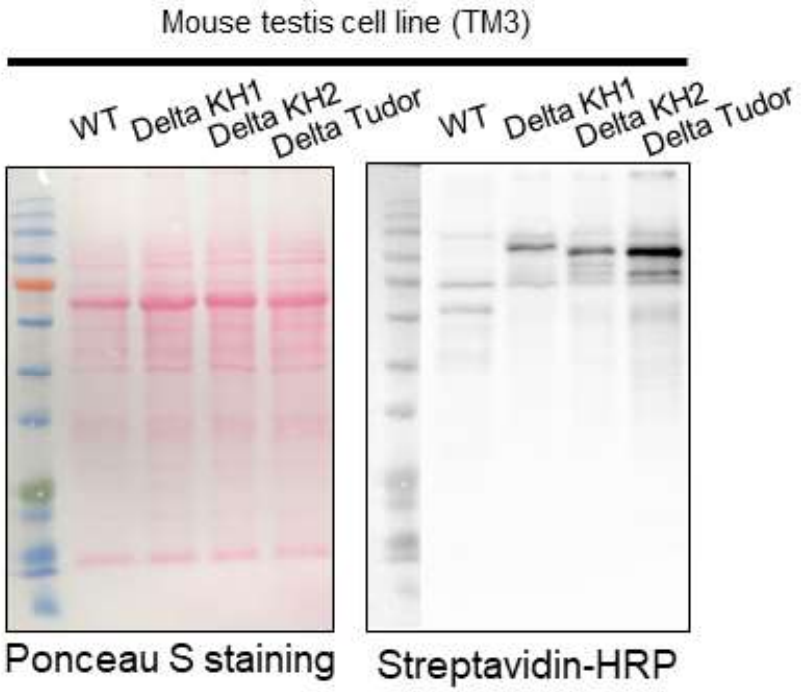

Supplementary Figure 2. Western blot analysis of TDRKH-deleted interactome by Spot-TurboID in mouse testicular cell (TM3)

국문 초록

Tudor and KH domain-containing protein (TDRKH)는 생식세포에서 piRNA precursor를 미토콘드리아로 가지고 오는 역할을 하는 것으로 알려져 있다. piRNA와 관련된 대부분의 연구는 생식세포에서 진행되어왔지만, TDRKH는 체세포와 암세포에서도 충분히 발현하는 것으로 알려져 있다. TDRKH의 상호작용체를 알아내기 위해서, 우리는 단백질 표지 기법, 그 중에서도 비특이적 biotin ligase인 TurboID를 TurboID의 C말단에 붙여 분석을 진행하였다. TDRKH-TurboID의 미토콘드리아로 발현을 발견하고 나서, 우리는 Spot-BioID의 분석 방법을 사용하여 TDRKH-TurboID로 인해 biotin이 표지 된 interactome을 분석하였다. 우리의 결과는 TDRKH가 mRNA 처리과정에 관여될 수 있음을 시사하고, 이 과정에서 미토콘드리아 표면의 RNA binding protein들과 함께 역할을 할 수 있다는 가능성을 제시한다. 또한 cytoskeleton 단백질들이 TDRKH와 interaction을 한다는 사실을 발견하였는데, 이 결과는 TDRKH가 transport process에 관여할 수 있다는 것을 의미한다. TDRKH의 interactome 중에서, HTT와 SNCA가 높게 발현하였으며 이는 뉴런 시스템과 관련된 단백질들이며, 각각 헌팅턴 무도증 및 파킨슨병과 관련된 단백질로 알려져 있다. 이 결과는 TDRKH와 관련된 것으로 보고된 유전적 운동신경병질, knockout 쥐에서의 표현형인 청성 뇌간반응과 관련될 수 있음을 시사한다. 또한 우리는 TDRKH의 각 도메인을 제거한 construct를 만듦으로써 도메인 특이적 상호작용체 분석을 진행하였는데, 이 결과를 통해서 SNCA는 TDRKH의 KH1 domain, SCRIB은 KH2 및 Tudor domain과 특이적으로 결합할 수 있음을 보였다.

.....

주요어 : TDRKH, 단백질체학, 단백질표지기법, TurboID, 미토콘드리아

학 번 : 2019-27124